Infrared Reflectivity of Pedestrian Mannequin for Autonomous Emergency Braking Testing

Terence Haran, *Senior Member IEEE* and Stanley Chien, *Senior Member IEEE*

Abstract - **In order to be able to evaluate the performances of different Autonomous Emergency Braking (AEB) systems for pedestrian crash avoidance and mitigation, a standard surrogate pedestrian mannequin needs to be developed. One of the requirements for pedestrian mannequin is to ensure it "looks" like a real representative pedestrian to each of the sensor modalities used in AEB systems. The purpose of this paper is to generate the recommended IR reflectance specifications for the standard surrogate pedestrian mannequin based on the collected data from various sources and the experiments.**

I. INTRODUCTION

Autonomous Emergency Braking (AEB) system will be standard or optional equipment on all vehicles in the near future. In order to evaluate and compare the performances of different AEB systems, standard test scenarios, methods and tools need to be developed. One essential testing tool needed is the surrogate pedestrian mannequin. There have been many ongoing efforts in developing the surrogate pedestrian mannequins [1-3] and several organizations (NHTSA, SAE, ISO, etc.) are creating mannequin standards. One of the requirements for pedestrian mannequin is to ensure it "looks" like a real representative pedestrian to LiDAR. However, to the best knowledge of the authors, there is not a published study that describes an infrared reflectivity specification to ensure that a pedestrian mannequin "looks" like a representative pedestrian to a LIDAR. The purpose of this paper is to derive the recommended IR reflectance specification for surrogate pedestrian mannequin based on the collected data from various sources and the experiments.

The paper is organized as follows: sections II specifies the problem in detail and provides background information. Section III describes the process for deriving the recommended IR reflectance of a pedestrian mannequin. Section IV describes the suggested measurement method for verifying IR reflectance. Section V concludes the paper. [1]

Terence Haran is with the Electro-Optical Systems laboratory, Georgia Tech Research Institute, Atlanta, GA 30332 USA. E-mail: terence.haran@gtri.gatech.edu.

Stanley Chien is with the Transportation Active Safety Institute, Indiana University - Purdue University Indianapolis, Indiana, USA. E-mail:schien@iupui.edu.

II. BACKGROUND INFORMATION

The goal of this paper is to specify the IR [2]reflectance of the pedestrian mannequin for testing the performance of pedestrian detection of automotive LIDAR. We first describe the common types of LIDAR used in automotive applications and then describe the LIDAR operation principles. It should be clarified that infrared wavelengths discussed here are in the near infrared portion of the spectrum rather than the far infrared wavelengths typically used for body heat detection.

A. Automotive LIDAR on the market

Optical sensor technology is finding increasing utility for applications involving navigation and obstacle avoidance. These sensors generally fall into two categories: passive sensors, which include typical visible band cameras, that collect light either from reflection of ambient light from objects in a scene or that is generated by thermal emissions from the objects themselves; and active sensors, which use their own light sources to "probe" a scene in order to determine information about its contents. Light detector and ranging (equivalently, laser detection and ranging), or LIDAR, sensors are a type of active optical sensor in which laser beams are used to interrogate a scene to determine the location and shape of objects within it. This is typically performed by illuminating some (or all) of the scene with a laser pulse of short duration (typically on the order of nanoseconds) and then precisely measuring the time required for the laser signal to be reflected back to its source, and in some cases the intensity of the reflected signal. These measurements allow the determination of how far an object is from the instrument (based on the time of flight for the reflected laser pulse) as well as how reflective the target is (based on the intensity of the received signal). LIDAR sensors are similar in concept to radar systems but utilize optical frequencies instead of radio frequency sources. There are numerous LIDAR system designs in use today which vary widely based on their intended applications, but most used for automotive applications obtain data over a two dimensional scene either by scanning a small laser beam rapidly across the scene and measuring the reflected signal with a single detector (thus obtaining range data at each "point" in the scene) or by using a large laser beam that illuminates the entire scene in one flash and then

measuring the reflected signal with a detector array that obtains numerous range points simultaneously.

The visible spectrum is part of the electromagnetic spectrum that is detectable to the human eye. The range of the wavelengths of visible light to a typical human eye is about 390 to 700 nm [4]. Human eye response can extend out to 750 nm wavelength for some individuals. It is undesirable to have LIDAR with visible lights installed on vehicles due to the potential for distraction as well as eye safety concerns associated with lasers. As a result, most automotive LIDAR systems use lasers that operate in the near-infrared portion of the electromagnetic spectrum. A search of the automotive LIDAR shows that most sensors operate in the wavelength range 785-1064 nm [5-9]. We have not found any specific automotive LIDAR examples operating under 785 nm. The data in Section 3 shows that IR reflectivity of common clothing material is high in the near-infrared wavelength range of 800-1200 nm.

B. LiDAR operation principle

Obtaining IR reflectivity measurements accurately requires accounting for numerous factors, including the characteristics of the intervening atmosphere as well as the geometry between the laser source, objects being interrogated, and the optical receiver. The basic laser range equation for a simplified LiDAR system is shown in equation (1), where P_{REC} represents the received power and P_T represents transmitted power, η represents the receiver quantum efficiency, R is the range to the target, A_{REC} is the area of the receiver, A_{TARGET} is the area of the target, Div_{TRANS} is the laser beam divergence before reflection, Div_{REF} is the laser beam divergence after reflection, and ρ represents the reflectance of the target. It should be noted that equation 1 neglects the effects of the intervening atmosphere between the LIDAR system and the targets in the scene and only captures the effects of the sensor and target behavior.

$$P_{REC} = P_T \cdot \frac{\eta}{\pi^2 R^4} \cdot \frac{A_{REC}}{Div_{TRANS}} \cdot \frac{\rho A_{Target}}{Div_{REF}} \qquad (1)$$

The reflected laser pulse can be detected if the received power as determined in equation (1) provides an adequate signal to noise ratio (SNR) when compared to the noise level of the receiver. The range to the target is not obtained from equation (1) but is determined by multiplying the time of flight required for the laser pulse to travel from its source to a target and for the reflected pulse to travel back to the receiver (usually co-located with the source) by the speed of light and then dividing by two (due to the round-trip travel). This relationship assumes that the time of flight has been measured accurately by the LIDAR system.

A quick analysis of the laser range equation indicates that the received power level is determined principally by the target reflectance properties, assuming that the LIDAR system parameters are fixed and range is treated as the independent variable. Therefore, it is better for the LIDAR to operate in a wavelength range where the targets of interest are more reflective.

The appropriate specification of target infrared reflectance is essential to ensuring proper performance testing of LIDAR sensors. Incident light on a particular medium is affected by a number of different phenomena, including refraction, reflection, absorption, diffraction, and diffusion, while it propagates through the medium. The net effect on the behavior of the light varies widely depending on the properties of that particular medium; however some portion of the light will be reemitted with a spectrum of reflectance that is unique to that medium. Reflectance is defined here as the ratio of the reflected flux to the incident flux at a given wavelength and for a given measurement geometry. For a laser beam incident on a target such as a pedestrian mannequin, the reflected signal will contain some percentage of the incident power and may also have a different divergence based on the geometry of the target. Reflectivity is a directional property, so if a beam of incident radiation is reflected strongly into a single direction (such as with a mirror), the reflection is called specular and the surface is described as glossy. When the radiation is reflected into all directions with a uniform distribution, the reflection is called diffuse and the surface is describes as lusterless. Illustrations of these cases are shown in the Figure 1(a). Most real surfaces fall somewhere between these two extremes.
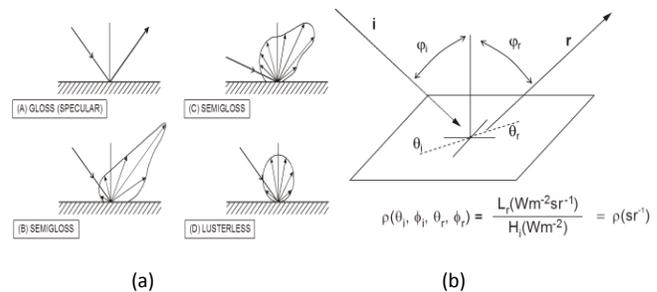

Figure 1. (a) Directional reflectivity examples and (b) bidirectional reflectance distribution function geometry.

It is important to note that reflectance is a bi-directional property that is dependent on the source, material, and observer geometry and can only be fully characterized by the Bi-directional Reflectance Distribution Function (BRDF) that describes reflectance for all combinations of source and observer angles as shown in Figure 1(b). These reflections are comprised of both a diffuse component, where reflections are scattered in all directions, and a specular component, where the light is reflected in accordance with Fresnel's law. If the BRDF is integrated over all angles, one can obtain the Total Hemispherical Reflectance (THR) for a sample. A surface that displays ideal diffuse reflectance where light is scattered equally in all directions is described as Lambertian. Diffuse reflectance is of particular interest for understanding the appearance of materials, since most naturally occurring surfaces, including fabrics, are diffuse reflectors. Assuming that clothing has diffuse reflectance properties significantly simplifies the testing process (by avoiding the need to test at numerous angles of incidence), but care must be taken to ensure that this assumption is valid in practice. This can be

accomplished by measuring the reflectance at several different angles of incidence and reflection for a particular material to confirm that the variation in reflectance as a function of angle is minimal. More samples are better, but at least nine combinations of incidence and reflectance angles should be measured. This allows the measurement of three different reflection angles for each of three angles of incidence. For a Lambertian reflector, these measurements should indicate that the reflectance at any combination of incidence and reflection angle does not vary by more than +/- 20% from the value measured at the normal angle of incidence and reflection. These measurements should be performed on a representative sample of the material prior to using it in tests where Lambertian behavior is assumed.

III. Infrared Reflectivity for a Pedestrian Mannequin

Since the penetration depth of infrared light is on the order of micrometers, the IR reflectivity of pedestrians is determined by their skin and clothing. Here, we determine the IR reflectance of skin and clothing and specify the IR reflectance property for standard pedestrian mannequins.

A. IR reflectance of pedestrian mannequin skin

Human skin reflectivity in various spectrums has been measured numerous times [10, 11]. Jacquez showed that in the 800nm-1100 nm wavelength range, the IR reflectivity of white race skin is in the range from 0.44 to 0.60. Cooksey presented the similar results for white skin and also provided that for black race skin is in the range from 0.4-0.55, and that of Asian race skin is from 0.43 to 0.58. The results were consistent in different experiments. Therefore, we recommend that the IR reflectance of the surrogate pedestrian mannequin skin to be in the range between 0.4 and 0.6.

B. IR reflectance of clothing fabric

As will be shown later in the paper, the IR reflectivity of clothing is a function of wavelength, fabric material, fabric color, and fabric weaving method. According to [12, 13], natural material cotton and manmade material polyester are the most common clothing material (especially for male clothing). Based on the clothing color analysis for pedestrians in TASI 110 car naturalistic study [14], the representative color for adults upper clothing is black (RGB=43, 41, 44), for adults lower clothing is deep dark blue (RGB=43, 44, 53), for children upper clothing is black (RGB=48, 46, 48), and for children lower clothing is medium blue (RGB=65, 71, 88). So the next problem is to determine the corresponding IR reflectivity for the common cloth fabric material in these color ranges.

When specifying the infrared reflectance for clothing used on the pedestrian mannequin, it is necessary to consider that the dyes used to give fabrics color are formulated for the visible portion of the spectrum (400-700 nm) and may have different properties at longer wavelengths where typical LIDAR systems operate. In addition, fabrics are actually comprised of layers of fibers, and depending on the thickness of the fabric and the density of the fibers, there may be some amount of reflection from the substrate underneath the fabric (e.g. skin or a different fabric) and therefore the apparent reflectance would represent the contributions from multiple layers. We measured 98 samples of cotton and polyester fabric in a wide variety of color with a variety of patterns from two vendors who supply fabric to the clothing industry [15]. These measurements were made using a Cary 5E spectrophotometer with the diffuse reflectance accessory installed over a wavelength range of 400 to 2000 nm with an interval of 1 nm. The instrument was first baselined by measuring the reflectance of a reference sample comprised of a Lambertian Spectralon coating with near 100% reflectance across the whole spectral region. This was followed by measurement of a zero baseline where the sample holder was empty. The test article was then installed in the sample holder and its spectrum was recorded by the spectrophotometer and calibrated based on the the reference sample and zero baseline measurements. The full procedure is described in reference [15].

The description of the fiber samples are listed in Table 1. Figures 3 and 4 plot the percentage reflectance versus wavelength for a variety of samples of cotton and polyester fabric. It is readily apparent from this data that the reflectance values can change dramatically at wavelengths above 700 nm and are not necessarily consistent at longer wavelengths either. The reflectance changes significantly between wavelengths 700-800 nm for most fabrics. The reflectivity of most fabric are relatively stable in the wavelength range 800-1200nm. It is also apparent that reflectance values can vary significantly from sample to sample, even at a particular wavelength.

The median and standard deviation of the measured reflectance values of all samples at 50 nm intervals in 700-1100 nm (in which most automotive LiDAR operate) are shown in Table 2. The samples displayed a one-sigma range of reflectance values from approximately 41% to 75% in wavelength range 800-1100nm.

TABLE I.   Description of fabric samples used for IR reflectance measurements. Measured reflectance at 750 nm and band-averaged reflectance and standard deviation between 800-1100 nm are shown for each sample.

Code	Name	Color	Type	Material	750 nm	800-1100 nm
20699	Wailea Coast Sun Swatch	Ebony	Art	Cotton	11	12 ± 0.95
20771	Orchid Cove Sun N Shade Swatch	Black	Art	Cotton	3	4 ± 0.36
25929	African Print Swatch	Multi animal print	Art	Cotton	37	55 ± 1.37
26491	African Print Swatch	Blue Orange Black Whi	Art	Cotton	54	62 ± 0.29
27401	Western Style Swatch	Multi-colored on Red	Art	Cotton	69	69 ± 0.40

27735	African Print Swatch	Burg, green blue blac	Art	Cotton	48	53 ± 0.18
27885	Colorful Sneakers Swatch	Multi-colored on Turq	Art	Cotton	48	63 ± 0.36
27888	Sassy Sealife Swatch	Blue and Orange on Gr	Art	Cotton	51	62 ± 0.44
27896	Hawaiian Print Swatch	Yellow Orange Green R	Art	Cotton	60	61 ± 0.19
29852	Rocket Ships Swatch	Multi Brights on Blac	Art	Cotton	45	61 ± 1.16
32787	Dolphins Swatch	Shades of Blue	Art	Cotton	51	63 ± 0.55
34181	African Animals Swatch	Multi	Art	Cotton	49	57 ± 1.93
34580	Cotton Flannel Print Swatch	Multi on Blue	Art	Cotton	48	55 ± 2.31
34851	Patriotic Print Swatch	Red/White/Blue/Black	Art	Cotton	48	54 ± 2.00
34869	Hawaiian Print Swatch	Multi	Art	Cotton	32	41 ± 0.49
35634	All Sports Swatch	Multi on Navy	Art	Cotton	27	37 ± 1.34
35979	Color Quake Swatch	Multi on Shades of Pu	Art	Cotton	38	42 ± 0.40
35988	Hawaiian Sunset Swatch	Multi	Art	Cotton	46	55 ± 2.77
35989	American Heritage Swatch	Multi	Art	Cotton	57	60 ± 0.58
36267	Lahaina Swatch	Black	Art	Cotton	4	4 ± 0.08
36476	Hawaiian Print Swatch	Multi on Green	Art	Cotton	52	57 ± 0.32
36477	Hawaiian Print Swatch	Multi on Red	Art	Cotton	54	57 ± 0.54
36495	Ropin Swatch	Multi on Tan	Art	Cotton	54	56 ± 0.49
36832	Surboard Collection Swatch	Multi on Pink	Art	Cotton	55	55 ± 0.44
26460	African Print Swatch	Red, Green, Black,Yel	Patterned	Cotton	57	59 ± 0.31
26474	African Print Swatch	Yellow Green Black Or	Patterned	Cotton	32	46 ± 1.48
26690	Cotton Polka Dots Swatch	Black with White dots	Patterned	Cotton	35	57 ± 1.98
26696	Cotton Polka Dots Swatch	Multi-colored on Blac	Patterned	Cotton	57	57 ± 0.37
26729	Cotton Polka Dots Swatch	Royal Blue/White	Patterned	Cotton	63	68 ± 0.23
26754	Cotton Polka Dots Swatch	Blue Red Yellow White	Patterned	Cotton	58	59 ± 0.41
31809	Seersucker Shirting Swatch	Pink, Green, Yellow	Patterned	Cotton	51	56 ± 0.43
34668	Camouflage Twill Swatch	Brown/Tan/Khaki	Patterned	Cotton	25	47±11.18
34671	Camouflage Print Swatch	Digital	Patterned	Cotton	51	61 ± 3.80
34856	Patriotic Print Swatch	Red/White	Patterned	Cotton	56	58 ± 0.52
35197	Seersucker Shirting Swatch	Turquoise/Navy Check	Patterned	Cotton	33	54 ± 1.96
35645	Cotton Flannel Print Swatch	Multi	Patterned	Cotton	61	69 ± 0.68
35811	African Print Swatch	Green/Red/Black/Purpl	Patterned	Cotton	42	55 ± 1.24
36364	Seersucker Shirting Swatch	Pink/Purple Plaid	Patterned	Cotton	59	59 ± 0.53
37368	Retro Dots Swatch	Blue/Lime/Ivory	Patterned	Cotton	60	62 ± 0.20
37665	Camouflage Print Swatch	Blues	Patterned	Cotton	15	19 ± 0.56
29982	Cotton T-Shirt Knit Swatch	Prism Violet	Solid	Cotton	66	72 ± 0.20
29995	Cotton T-Shirt Knit Swatch	chintz rose	Solid	Cotton	78	77 ± 0.66
29999	Cotton T-Shirt Knit Swatch	Blue Bell	Solid	Cotton	69	69 ± 0.25
30004	Cotton T-Shirt Knit Swatch	Chili Pepper	Solid	Cotton	67	70 ± 0.61
30008	Cotton T-Shirt Knit Swatch	Pastel Blue	Solid	Cotton	71	71 ± 0.26
30009	Cotton T-Shirt Knit Swatch	Sunkist Coral	Solid	Cotton	68	68 ± 0.26
30013	Cotton T-Shirt Knit Swatch	Pale Banana	Solid	Cotton	68	68 ± 0.24
31163	Cotton T-Shirt Knit Swatch	Black	Solid	Cotton	47	67 ± 1.12
36411	Cotton Interlock Swatch	Lime	Solid	Cotton	62	66 ± 0.66
36412	Cotton Interlock Swatch	Stop Sign	Solid	Cotton	68	69 ± 0.20
36413	Cotton Interlock Swatch	Royal Blue	Solid	Cotton	42	59 ± 8.45
20764	Tangier Sun N Shade Swatch	Sage	Art	Polyester	52	53 ± 0.99
28276	Seaside Lily Sun N Shade by Wa	Key Lime	Art	Polyester	54	68 ± 0.35
28277	Isla Bonita Sun N Shade by Wav	Ocean	Art	Polyester	65	70 ± 0.42
28278	Wailea Coast Sun N Shade by Wa	Flax	Art	Polyester	70	72 ± 0.65
28282	Essence Sun N' Shade Waver1	Onyx	Art	Polyester	24	23 ± 2.35
33785	Sadie Swatch	Azalea	Art	Polyester	54	57 ± 0.54
33787	Whim Swatch	Mist	Art	Polyester	64	64 ± 1.42
33788	Curvature Swatch	Foliage	Art	Polyester	25	30 ± 2.19
33793	Fiji Swatch	Midnight	Art	Polyester	31	31 ± 2.99
33796	Jefferson Swatch	Café	Art	Polyester	29	29 ± 1.10
20766	Biscayne Bay Sun N Shade Swatch	Dune	Patterned	Polyester	41	46 ± 0.84
20769	Rodeo Drive Sun N Shade Swatch	Sea Spray	Patterned	Polyester	29	31 ± 1.04
20770	Beach Umbrella Sun N Shade Swatch	Pink/Black	Patterned	Polyester	67	67 ± 0.69
20772	Marina Del Ray Sun N Shade Swatch	Surf	Patterned	Polyester	25	47 ± 4.99
28279	Beach Umbrella Sun N Shade by	Flax	Patterned	Polyester	23	27 ± 0.80
33794	Bistro Stripe Swatch	Midnight	Patterned	Polyester	45	46 ± 1.15
33799	Larrabee Swatch	Mocha	Patterned	Polyester	18	19 ± 0.81
36268	La Jolla Stripe Swatch	Aqua	Patterned	Polyester	51	54 ± 0.57
28280	Sunburst Sun N Shade by Waver1	Chocolate	Solid	Polyester	51	75 ± 0.91
31039	Polyester Shantique Swatch	Lilac	Solid	Polyester	69	68 ± 0.33
31498	Polyester Charmeuse Swatch	Ocean	Solid	Polyester	59	58 ± 0.48
32750	Polyester Charmeuse Swatch	Poppy	Solid	Polyester	63	61 ± 0.41
33512	Polyester Charmeuse Swatch	Canteloupe	Solid	Polyester	57	59 ± 0.57

| 33907	Polyester Poplin Swatch	White	Solid	Polyester	72	72 ± 0.25
33908	Polyester Poplin Swatch	Ivory	Solid	Polyester	56	55 ± 0.38
33909	Polyester Poplin Swatch	Gray	Solid	Polyester	69	70 ± 0.21
33910	Polyester Poplin Swatch	Green	Solid	Polyester	24	70 ± 1.86
33911	Polyester Poplin Swatch	Black	Solid	Polyester	49	69 ± 0.76
33912	Polyester Poplin Swatch	Copen	Solid	Polyester	69	70 ± 0.25
33913	Polyester Poplin Swatch	Burgundy	Solid	Polyester	68	71 ± 0.53
33914	Polyester Poplin Swatch	Royal Blue	Solid	Polyester	52	68 ± 2.21
34661	Polyester Poplin Swatch	Champagne	Solid	Polyester	57	57 ± 0.43
34662	Polyester Poplin Swatch	Banana	Solid	Polyester	56	56 ± 0.51
34705	Sunburst Sun N Shade Swatch	Keylime	Solid	Polyester	51	74 ± 3.33
35203	Polyester Poplin Swatch	Light Blue/Navy Cross	Solid	Polyester	34	58 ± 3.31
35204	Polyester Poplin Swatch	Tan/Brown Crossdye	Solid	Polyester	33	58 ± 3.81
36277	FR Poplin Swatch	Chili	Solid	Polyester	72	73 ± 0.24
36282	FR Poplin Swatch	Pistachio	Solid	Polyester	74	74 ± 0.23
36342	Polyester Poplin Swatch	Navy	Solid	Polyester	48	56 ± 0.25
36343	Polyester Poplin Swatch	Hunter	Solid	Polyester	51	55 ± 0.37
36344	Polyester Poplin Swatch	Red	Solid	Polyester	56	56 ± 0.38
37140	Polyester Charmeuse Swatch	Sunshine Yellow	Solid	Polyester	49	51 ± 0.32
37141	Polyester Charmeuse Swatch	Cyan	Solid	Polyester	39	61 ± 0.61
37701	Polyester Poplin Swatch	Mango	Solid	Polyester	56	56 ± 0.42
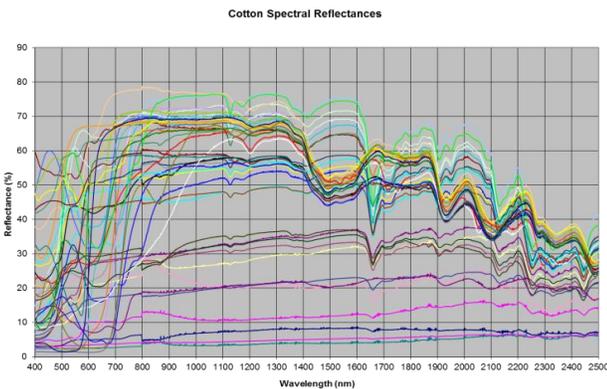
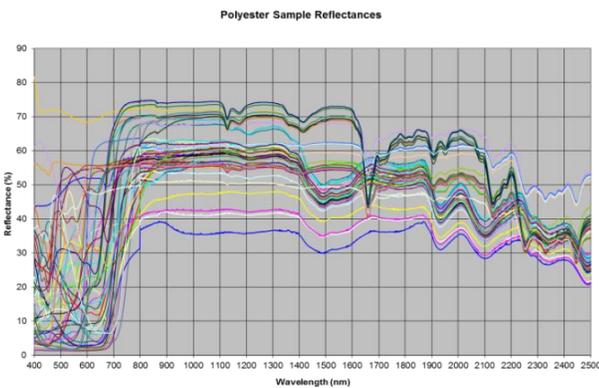Figure 2. Measured spectral total hemispherical reflectance for cotton samples.

Figure 3. Measured spectral total hemispherical reflectance for polyester samples.

Therefore, we recommend the IR reflectance of the pedestrian mannequin clothing fabric be specified as the median ± (0.75 Sigma) based on the measured samples. In other words, we recommend that the IR reflectance is between 46-70% in the wavelength range from 800 to 1100nm and between 40 and 64% in the range from 750 to 800nm. In addition, the fabric shall be sufficiently thick such that it does not transmit any light through to the substrate of the mannequin that could result in a different apparent reflectance.

TABLE II.   REFLECTANCE STATISTICS OF ALL MEASURED SAMPLES

Wavelength (nm)	Median Reflectance (%)	Standard Deviation (%)	One-Sigma Range (%)
700	42	20	22-62
750	52	17	35-69
800	57	16	41-73
850	58	16	42-74
900	58	16	42-74
950	58	16	42-74
1000	59	16	43-75
1050	59	16	43-75
1100	59	16	43-75

IV. IR REFLECTANCE MEASUREMENT METHODS

The IR reflectance of the standard pedestrian mannequin should be measured to ensure it satisfies the specifications. The diffuse reflectance of the fabric selected shall be measured versus wavelength using a spectrophotometer (such as a Cary 5E) using the procedure described in Section III.B. These instruments typically use a broadband light source and diffraction gratings to produce monochromatic light that illuminates a sample. The reflected light is then collected using an integrating sphere (usually part of a diffuse reflectance accessory) which measures all of the light reflected from the sample regardless of the reflection angle. This measurement is then compared to the measurement for calibrated samples to determine an absolute reflectance value which describes the total hemispherical reflectance of the sample.

In addition to measuring the diffuse reflectance, the BRDF of the sample at several discrete wavelengths should also be measured. These measurements shall not deviate by more than 20% from the value measured at the normal to the sample for a fabric that is a diffuse reflector. The BRDF is measured by illuminating a sample with a source placed at a particular incidence angle and then measuring the reflected light with a sensor placed at a known reflection angle. The wavelength of the illumination source is limited to a particular value through use of narrow band filters. This process is repeated for several different combinations of angles of incidence and reflection to fully characterize the BRDF. When samples are isotropic about their normals, it is not necessary to vary the incident azimuth. If the sample has surface structure that exhibits a preferred (as opposed to random) direction, the BRDF may vary significantly as a function of incidence angle; in this case BRDF measurements at several incident azimuth angles are required to fully characterize such a sample. The discrete values of a relative BRDF serve to characterize the reflectance of the sample. These relative BRDFs are then integrated and equated to the directional reflectance measured at the same incidence angle. This yields an absolute BRDF [16].

For situations where in situ measurements are required or preferred, infrared reflectance can also be measured using a portable spectrometer such as an Ocean Optics Jaz Spectrometer (http://oceanoptics.com/ product/jaz-spectrometer/) as described in the EAMA Articulated Pedestrian Target Specifications [2]. Before the start of the measurement, the device must be calibrated with a NIST-traceable reflection standard with a reflectance of 99%. The calibration should then be verified using reflectance standards with reflectance of 25% and 50%. The measurement shall be conducted with a special reflectance attachment which ensures a defined distance and angle between the probe and target. The measurement shall be performed at three separate points on the target with measurements taken at 45° and 90° for each point. The average of the three measurements at each angle will determine the reflectance for that material. The measured value at 45° shall not differ by more than 20% from the value measured at 90° to ensure diffuse behavior of the fabric.

V. CONCLUSION

The surrogate pedestrian mannequin is an essential tool for the performance evaluation of pedestrian autonomous emergency braking system. The IR reflectivity of the visible skin and clothing of the mannequin need to represent that of real pedestrians. This paper described a process and method to determine the IR reflectance of pedestrians and recommended the IR reflectance range for the standard surrogate pedestrian mannequin for AEB performance testing is between 46-70% in the wavelength range from 800 to 1100nm and between 40 and 64% in the range from 750 to 800nm. These values will ensure that the pedestrian mannequin reflectance will be representative of actual pedestrians that might be encountered by an AEB system in real world situations. As AEB usage becomes more widespread, continuous data collection and monitoring of fabric samples should be performed to ensure that these standards continue to be representative of pedestrian reflectance as new materials are introduced and clothing trends evolve.

REFERENCES

[1] Qiang Yi, Stanley Chien, et. al, "Mannequin Development for Pedestrian Pre-Collision System evaluation," 17th IEEE Int. conf. on Intelligent Trans. Sys., Oct 8-11, 2014, Qingdao, China.

[2] "Articulated Pedestrian Target Specifications Version 1.0", European Automobile Manufacturers Association, Oct 2015.

[3] Heath Albrecht, "Pedestrian Test Mannequins Objective Criteria for Evaluating Repeatability and Accuracy of PCAM Systems," http://www.nhtsa.gov/DOT/NHTSA/NVS/Public%20Meetings/SAE/2 015/Pedestrian%20Test%20Mannequins%20Objective%20Criteria(fin al).pdf (May 2016).

[4] Cecie Starr (2005). *Biology: Concepts and Applications*. Thomson Brooks/Cole.*ISBN 0-534-46226-X.*

[5] Velodyne HDL-64E Data Sheet, http://velodyneLiDAR.com/ docs/datasheet/63-9194_Rev-D_HDL64E_Data%20Sheet_Web. pdf , May 16, 2016.

[6] Eldada, Louay, "Today's LiDARs and GPUs Enable Ultra-accurate GPS-free Navigation with Affordable SLAM." 2014 GPU Technology Conference, San Jose, CA on March 27, 2014.

[7] Comparison of laser range scanners (LIDARs), http://www.phoenix-aerial.com/information/LiDAR-comparison (May 16, 2016).

[8] Trilumina LiDAR IR Laser Array Field, http://www.trilumina.com (May 16, 2016).

[9] Hokuyo Scanning Range Finder, https://www.hokuyo-aut.jp/02sensor/07scanner/urg_04ln.html (May 16, 2016)

[10] John A. Jacquez, John Huss, Wayne McKeehan, James M. Dimitroff, Hans F. Kuppenheim, "*Spectral Reflectance of Human Skin in the Region 0.7–2.6 µ,"* Zournal of Applied Physiology Published 1 November 1955 Vol. 8 no. 3, 297-299, http://jap.physiology.org/content/8/3/297.full-text.pdf+html

[11] Catherine C. Cooksey, Benjamin K. Tsai, and David W. Allen, "A collection and statistical analysis of skin reflectance signatures for inherent variability over the 250 nm to 2500 nm spectral range,", Proc. of SPIE Vol. 9082, 908206 · 2014, http://www.nist.gov/customcf/get_pdf.cfm?pub_id=916057

[12] Cotton from field to Fabric, https://www.cotton.org/pubs/ cottoncounts/fieldtofabric/upload/Cotton-From-Field-to-Fabric-129k-PDF.pdf (May 14, 2016)

[13] Cotton for Nonwovens: A Technical Guide. August 10, 2008]; Available from: http://www.cottoninc.com/product/ NonWovens/ Nonwoven-Technical-Guide/

[14] Libo Dong, Stanley Chien, David Good, Kai Yang, Yaobin Chen, Rini Sherony, and Hiroyuki Takahashi , "Determination of Pedestrian Mannequin Clothing Color for Evaluation of Pedestrian Pre-Collision Systems (PCS)," The 24th International Technical Conference on the Enhanced Safety of Vehicles (ESV2015), Gothenburg, Sweden on June 8-11, 2015.

[15] Haran, Terence, "Short-Wave Infrared Diffuse Reflectance of Textile Materials." Thesis, Georgia State University, 2008.

[16] B. P. Sandford, "Infrared Reflectance Properties of Aircraft Paints", AFGL-TR-84-0307, USAF Geophysics Laboratory, Hanscomb AFB, 1984.